N89-29863

2.5 TRANSPORT PROCESSES IN THE MIDDLE ATMOSPHERE: REFLECTIONS AFTER MAP

W. L. Grose

NASA Langley Research Center
Mail Stop 401B, Hampton, VA 23665-5225

The Middle Atmosphere Program (MAP) has provided a focus for considerable research on atmospheric radiative, chemical, and dynamical processes and the mutual coupling among these processes. In particular, major advances have occurred in our understanding of constituent transport as a result of near-global measurements obtained during MAP from several satellite-based instruments (e.g., LIMS, SAMS, SAGE, and SSU among others). Using selected portions of these data, we will review the development of progress in understanding transport processes with special emphasis on dynamically active periods. Examples will be presented which demonstrate coupling between chemistry and dynamics. In addition to the constituent data, we will review the use of Ertel's potential vorticity, inferred from satellite temperature data, as a diagnostic for interpreting transport phenomena. Finally, we will briefly illustrate the use of 3-D model simulations, in conjunction with the satellite data, for providing additional insight into fundamental transport mechanisms.

TABLE 1: Tracers and Their Domain for Transport Studies

Parameter	Comment
A. Middle and Upper Stratosphere	
N_2O, CH_4 (SAMS)	zonal mean only
O_3 (SBUV, LIMS, SAGE)	higher latitudes mainly
H_2O, nighttime NO_2 (LIMS)	four longitudinal waves for NO_2
Potential vorticity, PV (LIMS, SSU)	derived quantity
B. Lower Stratosphere	
N_2O, HNO_3, O_3 (LIMS)	six longitudinal waves
O_3 and aerosols (SAGE)	limited coverage per day
Aerosols (SME)	El Chichon dispersion
PV (LIMS and SSU)	derived quantity
$NO_y = HNO_3 + NO_2$ (LIMS)	appropriate for nighttime data only; four longitudinal waves
C. Total Column	
Ozone (TOMS, SBUV)	85 to 90% in stratosphere

E. E. Remsberg, 1987

TABLE 2. Uncertainties in Derived Quantities

- Instrument
- Sampling
- Inversion
- Synoptic Mapping
- Tie-on Level
- Geostrophic Approximation
- Numerical Differentiation

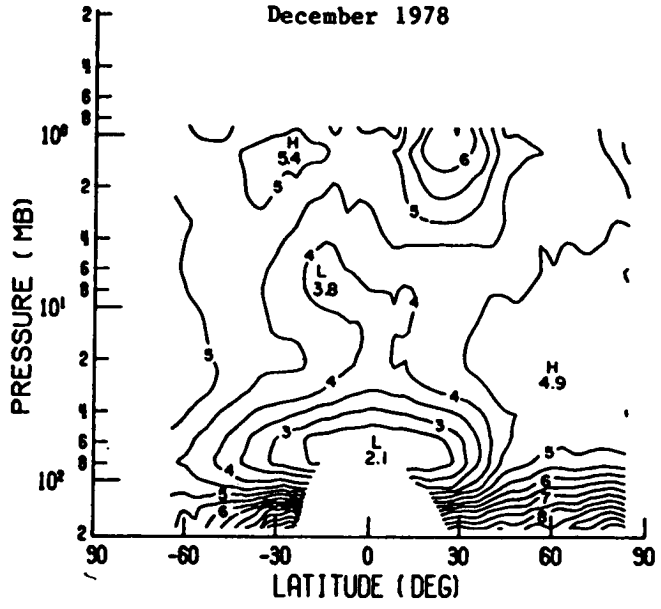

Figure 1. Zonal mean water vapor mixing ratio (ppmv) Nimbus 7 LIMS [Remsberg et al., 1984].

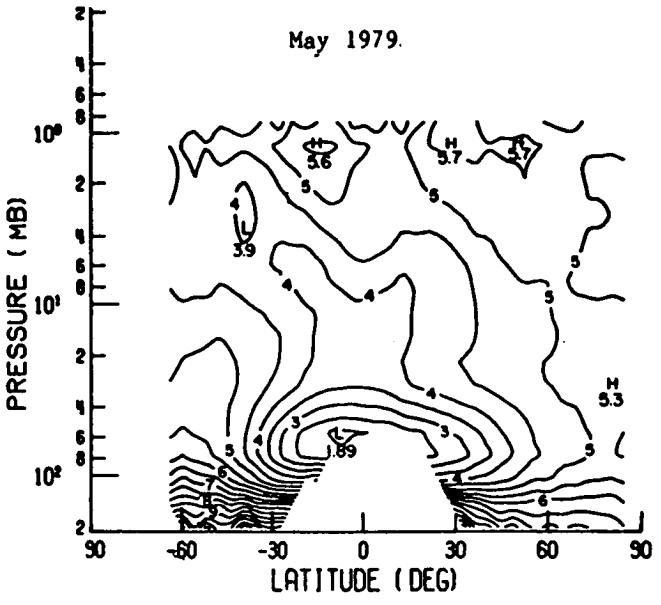

Figure 2. Zonal mean water vapor mixing ratio (ppmv) Nimbus 7 LIMS.

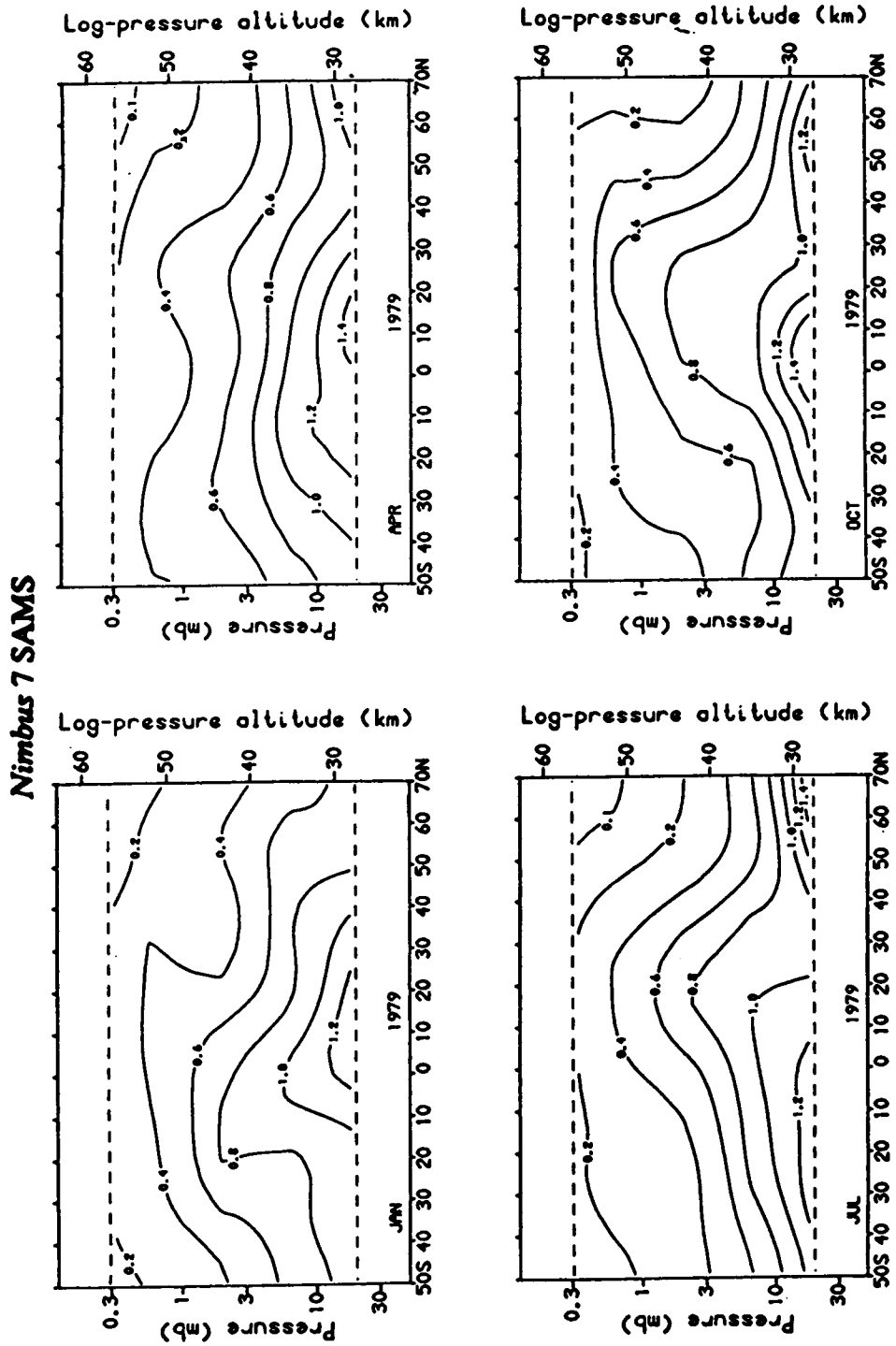

Figure 3. After Jones and Pyle [1984].

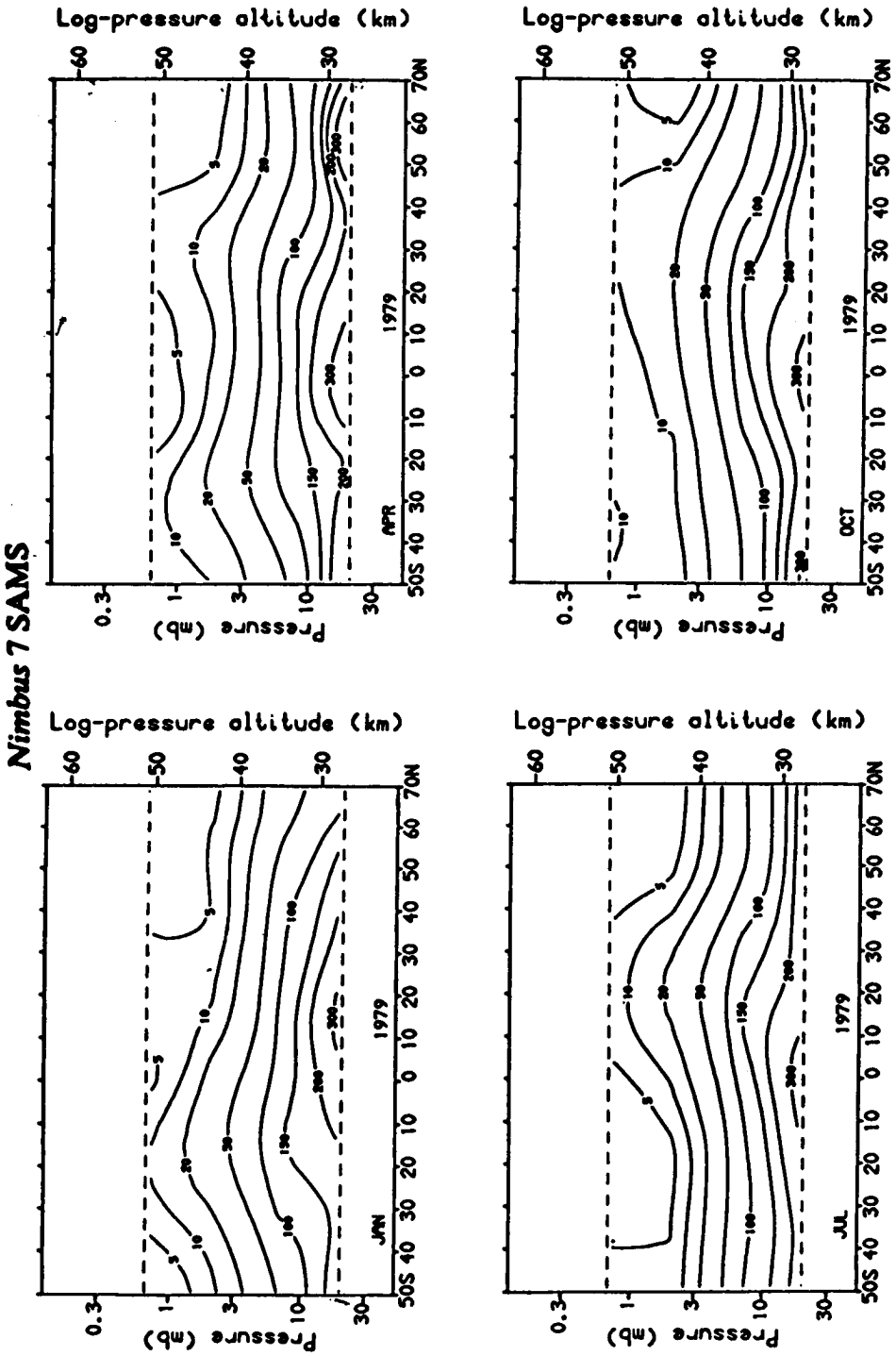

Figure 4. After Jones and Pyle [1984].

Diabatic Circulation Deduced from Satellite Observations

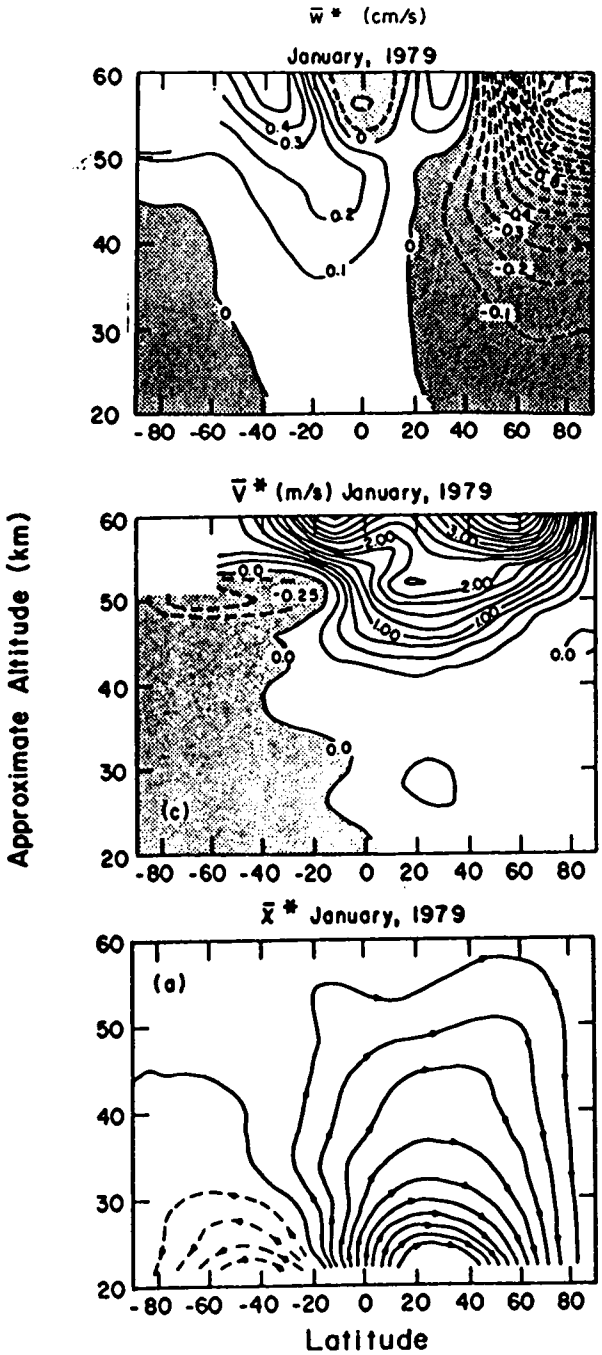

Figure 5. After Solomon et al. [*J. Atmos. Sci., 43*, 1986].

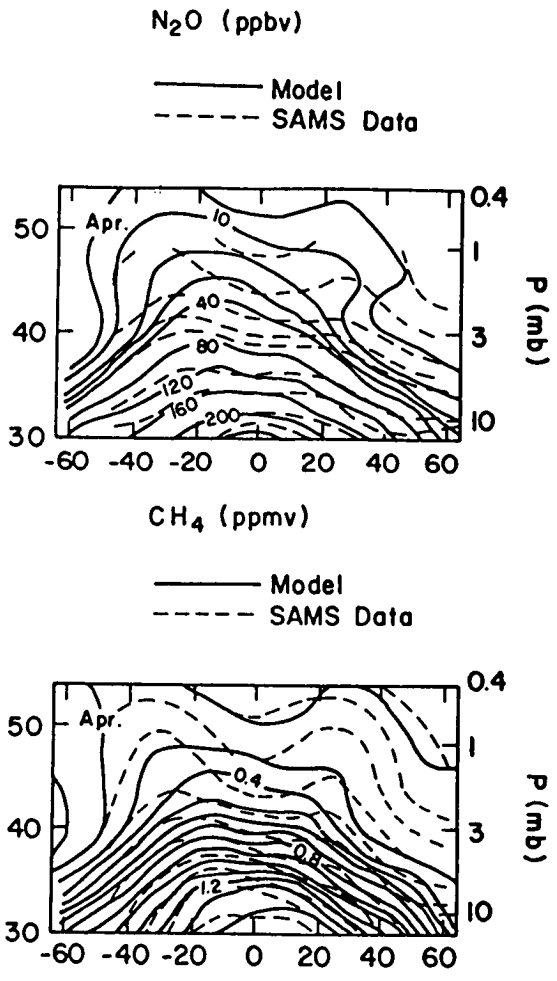

Figure 6. After Solomon et al. [*J. Atmos. Sci., 43,* 1986].

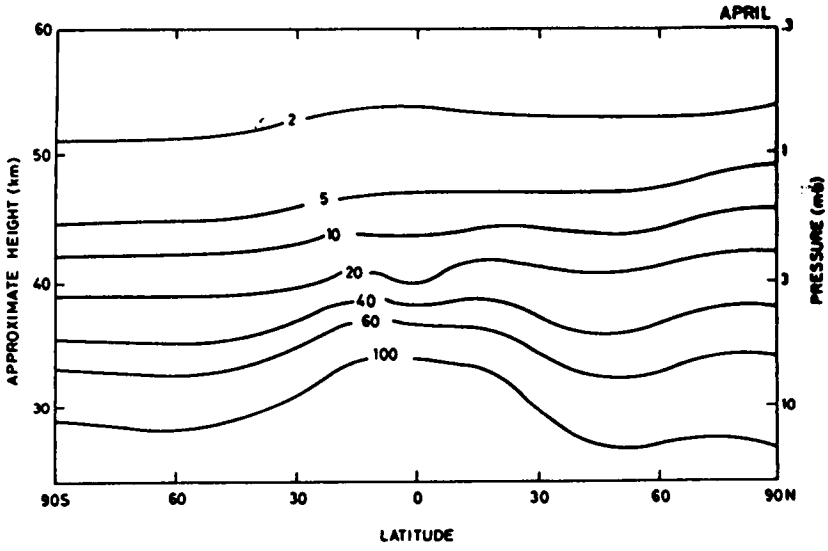

Figure 7. Monthly-averaged latitude-height cross section of N_2O volume mixing ratio (ppbv) for April from run B [Gray and Pyle, *Q. J. R. Met Soc.*, 1986].

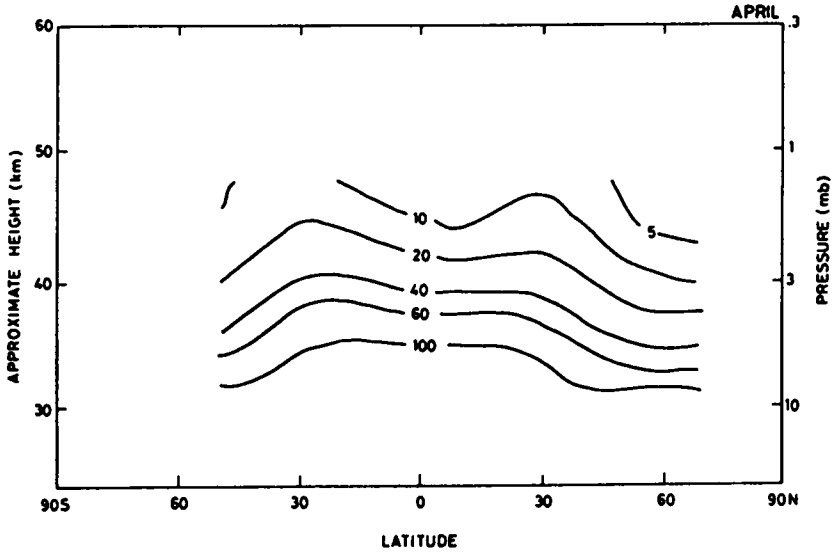

Figure 8. Monthly-averaged latitude-height cross section of N_2O volume mixing ratio (ppbv) for April 1979 from the SAMS satellite measurements [Gray and Pyle, *Q. J. R. Met Soc.*, 1986].

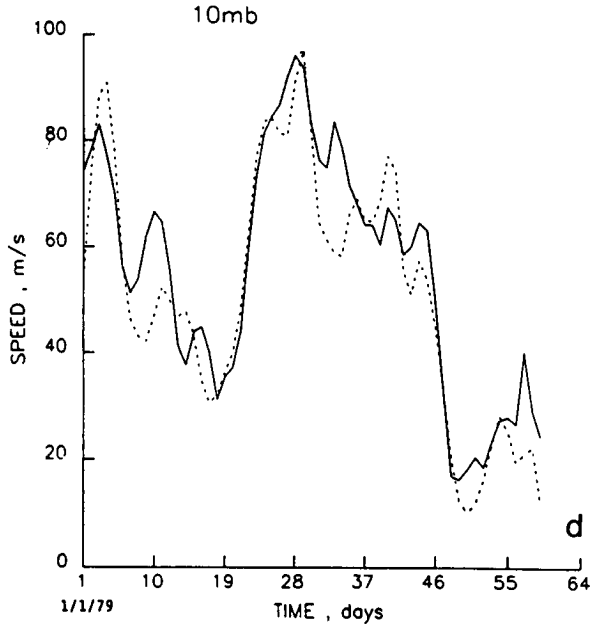

Figure 9. Time series comparison of horizontal wind speed (m/s) over Berlin between radiosonde 12 GMT measurements (dashed) and LIMS geostrophic values (solid) derived from the 12 GMT geopotential height map sequence. Analysis is for January 1 (day 1) to February 28 (day 59), 1979. Note that 50 mb values are derived from NMC heights.

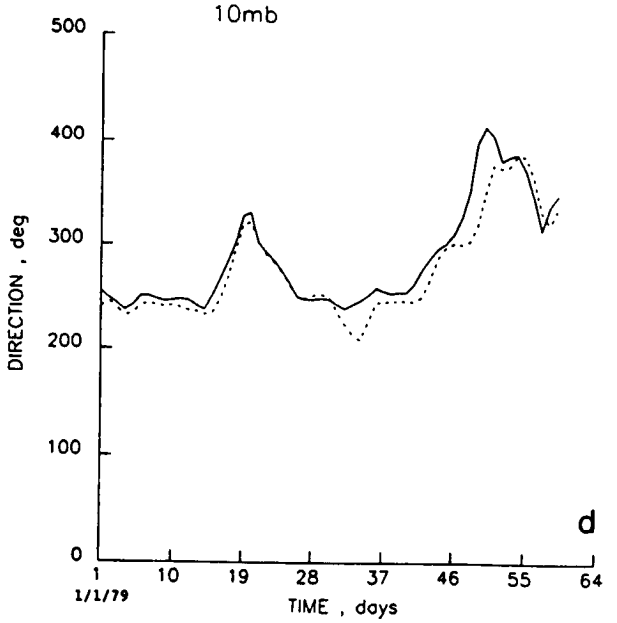

Figure 10. As in Figure 9, but for horizontal wind direction (deg). Values denote the phase of the wind vector over Berlin relative to true north (0°/360°), e.g., 270 deg = west to east airflow.

TRANSFORMED EULERIAN FORMULATION

$$\frac{\partial \bar{u}}{\partial t} - f\bar{v} + \frac{1}{r_o \cos^2\phi}\frac{\partial}{\partial \phi}(\cos^2\phi\ \overline{u'v'}) = 0$$

Momentum Equation

$$\frac{\partial \bar{\theta}}{\partial t} + \bar{\theta}_p\,\bar{\omega} + \frac{1}{r_o \cos\phi}\frac{\partial}{\partial \phi}(\cos\phi\ \overline{v'\theta'}) = \bar{Q}$$

Thermodynamic Equation

$$\tilde{F} = (F_\phi, F_p)$$

$$F_\phi = -r_o \cos\phi\ \overline{u'v'} \qquad F_p = f\, r_o \cos\phi \frac{\overline{v'\theta'}}{\bar{\theta}_p}$$

Eliassen-Palm Flux

$$\bar{\omega}^* = \bar{\omega} + \frac{1}{r_o \cos\phi}\frac{\partial}{\partial \phi}\left(\frac{\overline{v'\theta'}\cos\phi}{\bar{\theta}_p}\right) \qquad \bar{v}^* = \bar{v} - \frac{\partial}{\partial p}\left(\frac{\overline{v'\theta'}}{\bar{\theta}_p}\right)$$

$$\frac{\partial \bar{u}}{\partial t} - f\bar{v}^* = \frac{1}{r_o \cos\phi}\nabla \cdot \tilde{F}$$

Transformed Equations

$$\frac{\partial \bar{\theta}}{\partial t} + \bar{\theta}_p \bar{\omega}^* = \bar{Q}$$

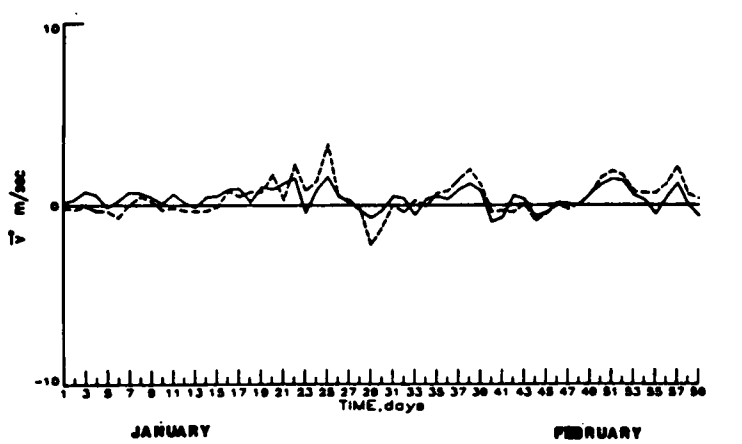

Figure 11. Residual meridional velocity (in units of ms^{-1}) inferred from the momentum equation and from the thermodynamic equation for January-February 1979 at 68°N latitude and 10 mb pressure (LIMS data).

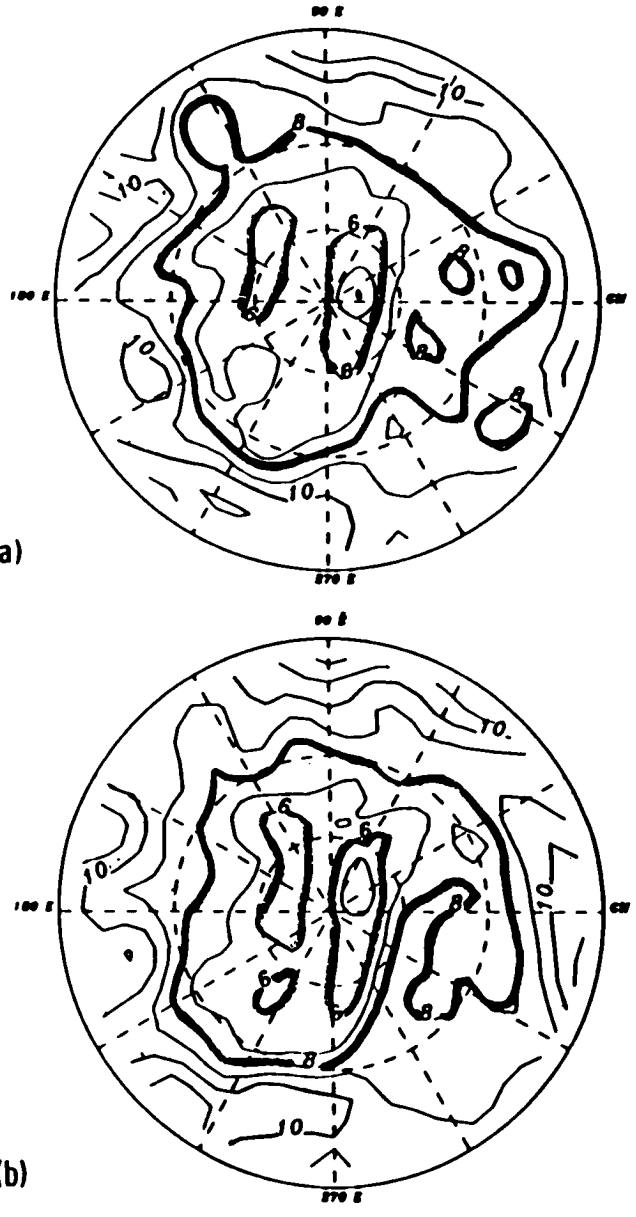

Figure 12. Ozone mixing ratio (ppmv) on the 10 mb pressure level of the Northern Hemisphere for the LaRC model simulation: (a) February 1, (b) February 3, (c) February 5, (d) February 7, and (e) February 9.

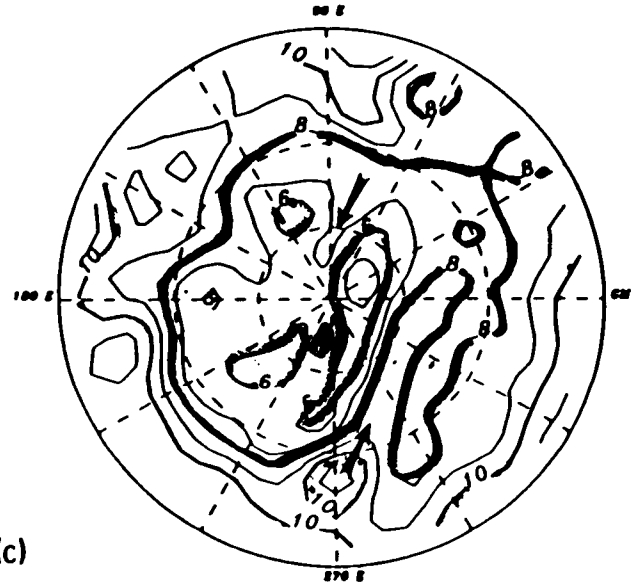

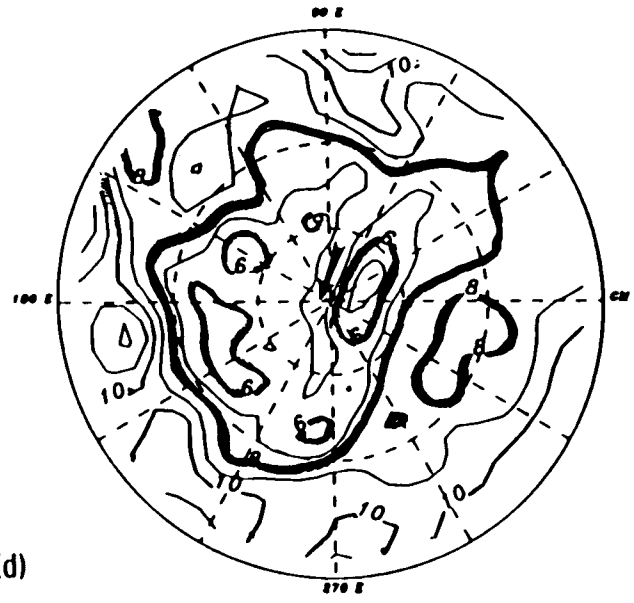

Figure 12 continued.

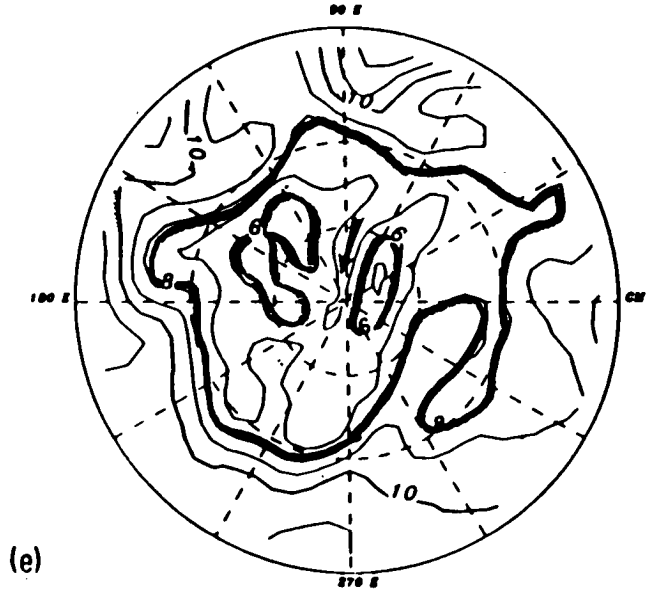

Figure 12 continued.

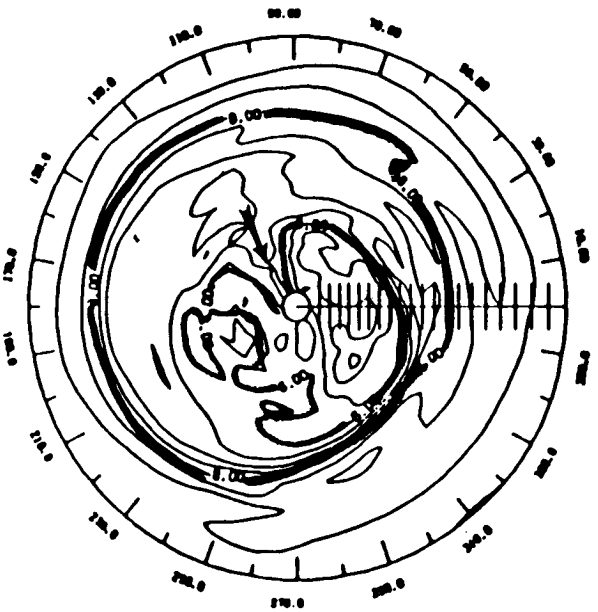

Figure 13. Ozone mixing ratio (ppmv) on the 10 mb pressure level of the Northern Hemisphere from the LIMS experiment, January 26, 1979.

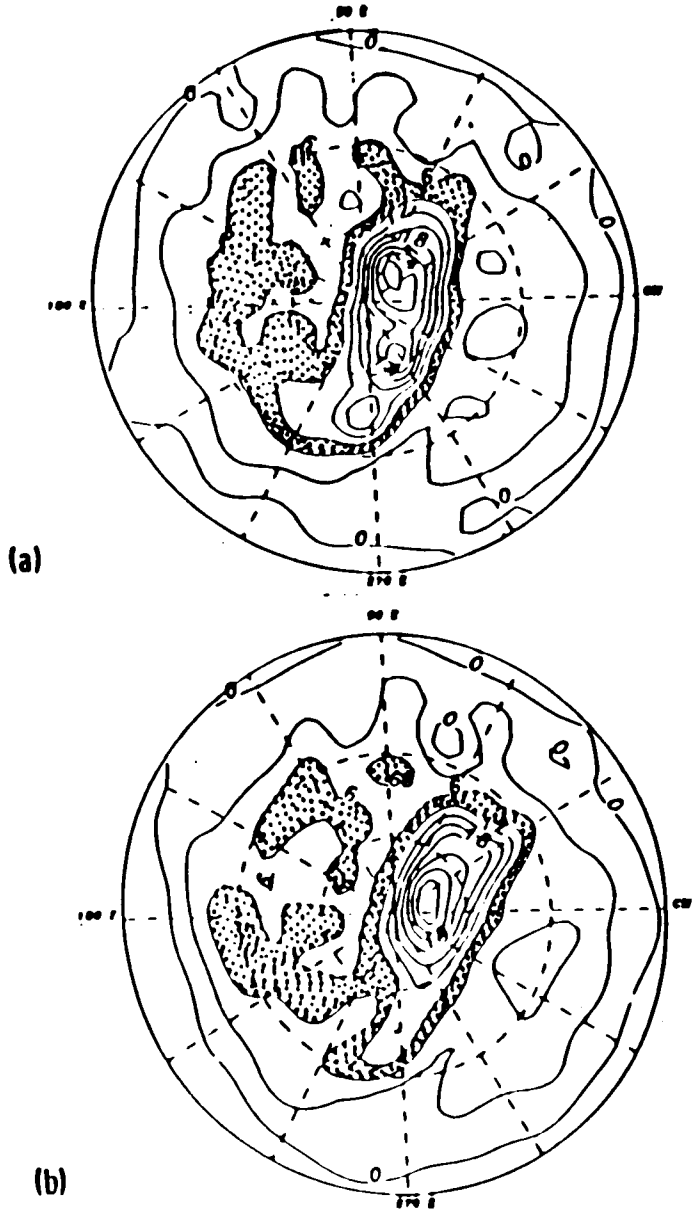

Figure 14. Ertel's potential vorticity 850 K N.H. LaRc 3-D model. (a) February 1; (b) February 7.

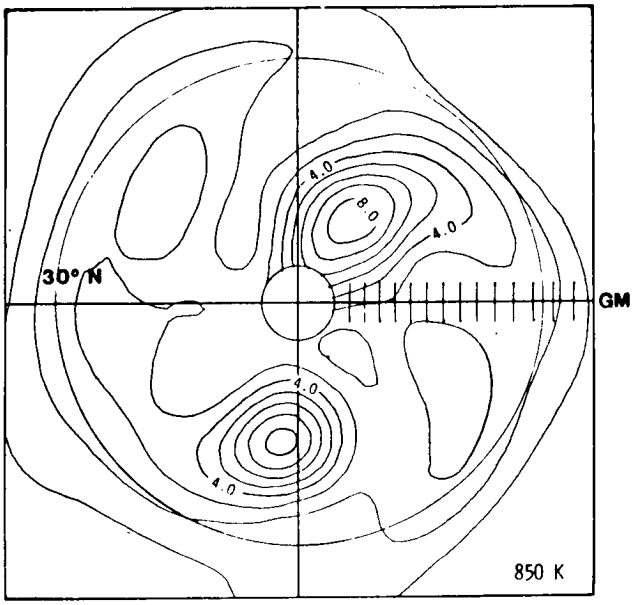

Figure 15. Ertel's potential vorticity ((K x M x M/(KG x S)) x 1.E–4) LIMS N.H. 25 February 1979.

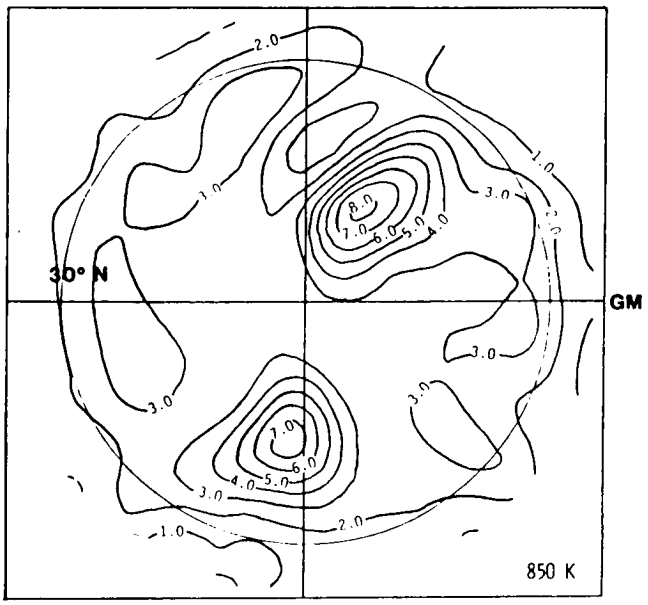

Figure 16. Ertel's potential vorticity ((K x M x M/(KG x S)) x 1.E–4) SSU N.H. 25 February 1979.

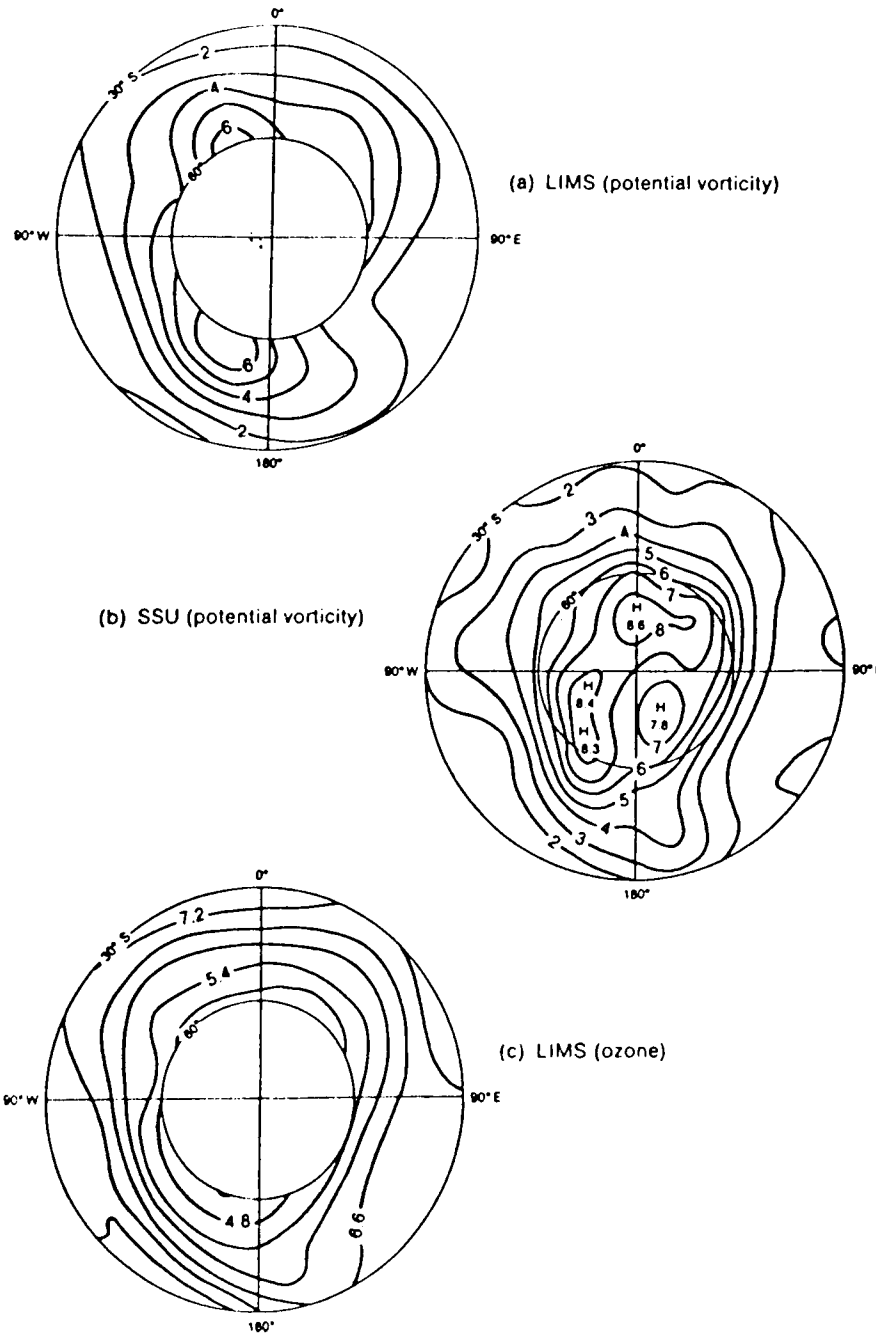

Figure 17. (a) LIMS and (b) SSU maps of modulus of Ertel's potential vorticity on the 850 K isentropic surface for the Southern Hemisphere on May 24, 1979. Units: 10^{-4} K m^2 kg^{-1} s^{-1}. (c) Ozone mixing ratio (ppmv) from LIMS on the 850 K surface on the same day.